Available online at www.dergipark.org.tr/en

INTERNATIONAL ADVANCED RESEARCHES
and
ENGINEERING JOURNAL

Journal homepage: www.dergipark.org.tr/en/pub/iarej

e-ISSN: 2618-575X

International Open Access

Volume 05
Issue 03

December, 2021

Research Article

Investigating the construction parameters of deep mixing columns in silty soils

Yavuz Yenginar [a,*]**, *Ahmed A.M.M. Mobark*** [b] ***and Murat Olgun*** [b]

[a] *Necmettin Erbakan University, Engineering Faculty, Department of Civil Engineering, 42090, Konya, Turkey*

[b] *Konya Technical University, Faculty of Engineering and Natural Sciences, Department of Civil Engineering, 42130, Konya, Turkey*

ARTICLE INFO

Article history:
Received 05 August 2021
Revised 26 November 2021
Accepted 10 December 2021

Keywords:
Cement
Deep soil mixing
Fly ash
Silty soil
Superplasticizer
Taguchi method

ABSTRACT

In the present research, the optimum condition of the grout consisting of cement, fly ash, superplasticizer, and water was determined to produce the most durable and impermeable deep mixing columns (DMC) on silty soils. It is aimed to reduce the grout cost and environmental pollution by using high-rate fly ash in the grout. Superplasticizer additive was used to increase the flow consistency of grout consisting of high-rate fly ash. The design of the experiments was made using the 5-parameter and 4-level L16 orthogonal array table specific to the Taguchi method. Accordingly, the unconfined compression strength (q_u) and the permeability coefficient (k) of the soil-binder mixtures at the end of the 7- and 28-days curing time were determined. According to the test results, regression analyzes were performed and models with high reliability were created for q_u and k. As a result of optimization studies, to produce DMC having high strength and low permeability, grout content should be consisting of 14% cement, 14% fly ash (ratio of fly ash in the binder is 50%), 2.68% super plasticizer additive, and 0.95 water/binder ratio. The pozzolanic reactions in soil-binder samples with different grout contents were examined by SEM analysis.

1. Introduction

All over the world, especially in city centers, most of the stable soil had already been used. The construction site requires a stable area of appropriate soil properties since weak soils have to be improved before the construction work. One of the methods used for stabilizing soils is the deep mixing method (DMM), defined as the mixing process of cement, lime, slag, and other binders with soil. DMM improves the soil properties in terms of geotechnical concerns such as bearing capacity, hydraulic conductivity, settlement, and horizontal displacement.

The effects of cement and other binders on soil-cement slurry have been investigated by lots of researchers. The unconfined compression strength (UCS) of the deep mixing column depends on binder dosage, curing period, curing temperature, and natural soil water content [1]. Increasing cement dosage from 100 kg/m^3 to 200 kg/m^3 gives 10 times higher compression strength, and there is a linear relation between UCS and cement dosage [2].

Since cement production is expensive and causes environmental pollution, the binder replacement method with a natural or by-product material may be useful for many cement-based constructions works. A common by-product material is fly ash generally used to create longer-lasting infrastructure in road constructions and embankments. Li et al. [3] found that the fly ash-soil samples had a strength between 940 kPa and 4300 kPa at the end of the 14-day cure period, whereas the soil alone had a strength of 317 kPa. Moreover, soil friction angles increased up to 2-3 times according to fly ash content. The optimum fly ash ratio for the mix was 60%. Since fly ash is a lightweight material, the higher percentage of fly ash decreases dry densities and increases optimum water content [4,5]. Increasing the amount of fly ash into soil reduces plasticity, hydraulic conductivity, and compressibility [6–9]. Although replacing cement with fly ash reduces cement cost and environmental pollution, fly ash additive materials have early strength problems but, the final compression strength is high [10]. Some minerals of silicon and aluminum in fly ash create a secondary reaction with the cement hydration products. Thus, the void ratio and permeability of the deep mixing column decreases. The UCS and elastic modulus of columns improved with increasing fly ash amount [11].

The injectability of the grouting mixture is important to obtain well-mixed columns. Although the higher water

* Corresponding author. Tel.: +90 507 857 9240.
E-mail addresses: yyenginar@erbakan.edu.tr *(Y. Yenginar)*, ahmeed696@yandex.com *(A.A.M.M Mobark)*, molgun@ktun.edu.tr *(M. Olgun)*
ORCID: 0000-0002-6916-4068 *(Y. Yenginar)*, 0000-0002-3989-641X *(A.A.M.M Mobark)*, 0000-0001-7856-8227 *(M. Olgun)*
DOI: 10.35860/iarej.978978

content in the grouting mixture makes grouting easier, it reduces the strength of soil-cement samples. Therefore, to increase the strength, the water content has to be reduced. Since grouting mixtures are pumped into the soil at the field, higher fluidity and low viscosity are achieved by raising the water/cement ratio and adding chemical additives. In different studies, water/cement ratios were used as following; 0.5-2 [12], 0.6-2 [13], and 1-3 [14]. Adding chemical additives impacts the fluidity of cementitious material even for mixtures with very low water/cement ratios. Achieving higher strength requires lower water/cement ratios. However, lower water content results in low fluidity. Thus, chemical additives are used to maintain a higher fluidity value for that low water content. The addition of superplasticizers into grouting mixtures, more viscous grout at lower water/cement ratio [15,16], and more strength and less permeable soil-cement mixtures can be obtained.

Full factorial or partial factorial design can be performed when examining the effects of parameters that are effective on any process [17]. Full factorial design can be applied when the number of parameters studied is small. However, as the number of parameters and their levels increases, full factorial design becomes very laborious and time-consuming. The partial factorial design also has its downsides [18]. Genicci Taguchi developed a statistical method [19–22] to determine the relationship between the parameters that affect the process and the results by making a few experiments, observations, or analyzes as possible. This method is used in many different fields [23–27]. The basic methodology of the Taguchi method consists of four steps: (1) determining the parameters and their levels that affect the process, (2) choosing an appropriate orthogonal index table, (3) performing the experiments and analyzing the results, and (4) obtaining and verifying the optimum results.

The purpose of this research is to determine the optimum grout content to obtain the highest strength and the lowest permeability of the soil-binder mixture representing the deep mixing column. Grouting consists of different amounts of cement, fly ash, superplasticizer, and water/binder ratio mixed with the silty soil whose consistency changes semi-solid to liquid form and cured for 7 and 28 days. The design of the experiments (DOE) was performed using the Taguchi method, which is a statistical method. Experimental results were analyzed using a factorial design to find the optimum grout content. The optimum design is controlled by validation tests (unconfined compression and permeability tests) and SEM images.

2. Materials and Methods

2.1 Soil

The soil was obtained from the Doğanhisar district located at Konya Province in Turkey. Liquid limit (w_L), plastic limit (w_p) and plasticity index (I_p) of soil determined as 31.3%, 18.1% and 13.2%, respectively. The soil is classified as ML according to USCS using Atterberg limits and grain size distribution curve given in Figure 1.

2.2 Grouting Materials

The grout consists of cement, fly ash, and superplasticizer. The main binder material in grout is Type I (42.5 R) Ordinary Portland Cement (OPC). Its chemical properties are given in Table 1. Since the fly ash gained strength over a long period, high early strength cement was used.

The fly ash was obtained from Aluminum Recovery Central in Seydişehir, Turkey. Fly ash is the petty binder material used to reduce cement costs inside the grout. The fly ash can be defined as high lime fly ash since its free lime content is 16.3% (Table 1). Most of its particles were in the silt size (84.2%) with light brown color.

The superplasticizer used in this study meets the requirements for water-reducing (Type A) and high range water-reducing (Type F) admixtures according to ASTM C 494/C 494M [28]. This additive maintains high plasticity in concrete for a longer time compared to traditional superplasticizers. In the plastic state, it extends slump retention, control set times, and minimizes bleeding water. On the other hand, in the hardened state, it provides higher earlier strength, increases ultimate compression strength, develops a higher modulus of elasticity, and decreases permeability.

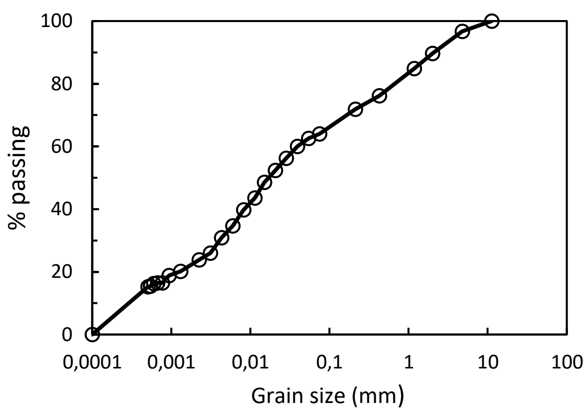

Figure 1. Grain size distribution curve of soil

Table 1. The chemical properties of cement and fly ash

Chemical composition (%)	Cement	Fly ash
SiO_2	22.1	19.8
Al_2O_3	5.3	8.1
Fe_2O_3	2.2	6
CaO	63.7	28.3
MgO	2.4	1
SO_3	3.1	18.2
Na_2O	0.12	0.1
K_2O	0.94	0.4
Free CaO	1.6	16.3
Loss on ignition	-	1.8

2.3 Design of Experiments (DOE)

Scientists systematically collect data and examine the relationship between input variables (factors) and output parameters (responses) that are effective on any process using the design of experiments (DOE) method. The Taguchi method is a robust DOE method used to optimize the parameters that affect the process. This method reduces the mean and variance of the process performance characteristics and allows obtaining high-quality analysis results with a few experiments. The first step in the Taguchi method is the selection of parameters and their levels.

In the present research, investigating parameters on column performance are amounts of cement, fly ash, superplasticizer, water/binder ratio in grout and water content of untreated soil. Parameters and their levels were given in Table 2. Taguchi's standard L16 (5^4) orthogonal array (OA), which consists of 5 factors and 4 levels, was used in the design of experiments (Table 3).

Unconfined compression strength (q_u) and permeability coefficient (k) values were used in the statistical analyzing process. In the first stage, Taguchi analysis was performed and S/N (signal-to-noise) ratios were obtained. S/N ratio refers to the distribution around the target value, and there are three categories for the performance characteristic: (1) larger the better, (2) smaller the better, and (3) nominal the better.

Table 2. Controllable factors and levels in Taguchi design

Levels	Parameters				
	C	F	A	w/b	w_n
1	3	0	0	0.9	20
2	7	5	1	1.1	24
3	11	10	2.5	1.3	28
4	15	15	4	1.5	32

Table 3. Design of experiment using Taguchi method (standard L16 orthogonal array)

Design	Parameters and their levels				
No	C	F	A	w/b	w_n
1	1	1	1	1	1
2	1	2	2	2	2
3	1	3	3	3	3
4	1	4	4	4	4
5	2	1	2	3	4
6	2	2	1	4	3
7	2	3	4	1	2
8	2	4	3	2	1
9	3	1	3	4	2
10	3	2	4	3	1
11	3	3	1	2	4
12	3	4	2	1	3
13	4	1	4	2	3
14	4	2	3	1	4
15	4	3	2	4	1
16	4	4	1	3	2

This study aims to manufacture a deep mixing column with high strength and low permeability. For this reason, S/N ratios were determined using Equation (1) of "larger the better" option for strength response and Equation (2) of "smaller the better" option for permeability response. In Taguchi analysis, the S/N ratio is used as the quality characteristic. Taguchi found that the mean and standard deviation are directly proportional to each other. This is the reason why the S/N ratio is used instead of the standard deviation. Each experiment was performed twice to reduce the effect of the uncontrollable factors. Statistical analyzes were made with Minitab software.

$$S/N = -10log_{10}\left(\frac{1}{n}\sum_{i=1}^{n}\frac{1}{Y_i^2}\right) \quad (1)$$

$$S/N = -10log_{10}\left(\frac{1}{n}\sum_{i=1}^{n}Y_i^2\right) \quad (2)$$

where Y_i is the response (output) of the i-th experiment and n is the repetition number of response characteristics.

In the second stage, the desirability function approach was applied to optimize all parameter levels including the curing period of deep mixing samples. Derringer and Suich [29] initially developed the idea of the desirability function approach. In this approach, all responses are transformed into the same scale of undesirable desirability (individual desirability) [30]. There are 3 different desirability functions $d_i(y_i)$ to obtain the response parameter y_i at the maximum, minimum, or target value. The individual desirability $d_i(y_i)$ can be calculated to minimize a response using "smaller better" formulas in Equation (3) and maximize a response using "larger better" formulas in Equation (4) [29,31]. Then, the geometric mean of individual desirabilities using Equation (5) gives the overall desirability D.

$$d_i(y_i) = \begin{cases} 1 & , y_i(x) < T_i \\ \left(\frac{y_i(x)-U_i}{T_i-U_i}\right)^r & , T_i \le y_i(x) \le U_i \\ 0 & , y_i(x) > T_i \end{cases} \quad (3)$$

$$d_i(y_i) = \begin{cases} 0 & , y_i(x) < L_i \\ \left(\frac{y_i(x)-L_i}{T_i-L_i}\right)^r & , L_i \le y_i(x) \le T_i \\ 1 & , y_i(x) > T_i \end{cases} \quad (4)$$

$$\mathrm{D} = \left(d_1(y_1) \times d_2(y_2) \times \ldots \times d_m(y_m)\right)^{1/m} \quad (5)$$

where x is the factors. L_i and U_i are lower and upper acceptable values of y_i, respectively, while T_i is target values desired for i^{th} response, where $L_i \le T_i \le U_i$. r is used to determine the shape of $d_i(y_i)$ and change between 0 and 1. m is the number of responses.

Desirability value changes between 0 and 1. A desirability value of 0 indicates that the predicted outcome value is outside of acceptable limits. A desirability value of 1 indicates that there is maximum agreement between factors and results, that is, maximum performance has been achieved. [32]. In the desirability function approach, the curing period was added to the L16 design table as the sixth parameter with two levels (7 and 28 days). Hence the number of trial mixes was increased to 32. Then, regression analysis and multi-response optimization was performed using the desirability function approach in Minitab software. All of the statistical analyzes were carried out considering the 95% confidence interval.

2.4 Preparing and Curing Specimens

Before preparing the soil-binder mixtures, the soil was dried at 60° in the oven and sieved through a 2 mm opening sieve. For each design, the amount of cement and fly ash were determined as a percentage of dry soil and all were mixed in the dry state (the dry mixture). The total water content of the mixture includes grouting water and soil's natural water content. Grouting water is calculated by multiplying the water/binder ratio and dry binder amount. The amount of superplasticizer was determined as the percentage of a dry binder. Then, grouting water, water from soil's water content, and superplasticizer mixed (the liquid mixture). After that, the liquid mixture was added step by step to the dry mixture to obtain a homogeneous mixture. The mixing process was done by a mixer and continued for at least 10 minutes for each mixture. After that, the mixture was cast in PVC molds having 50 mm inner diameter. The height of molds used for UCS and permeability tests were 100 mm and 30 mm, respectively. Fresh mixtures of soil-binder samples cast in molds were left at room temperature for 5-6 hours to harden and then cured in the curing pool by sealing. The curing period of samples was 7 and 28 days.

3. Results and Discussion

3.1 Unconfined Compression Strength (UCS) Test

Unconfined compression strength tests were performed according to ASTM-D2166/D2166M [33]. The cylindrical soil-binder sample is loaded axially at an axial strain rate between 0.5 to 2%/min. The unconfined compression strength (q_u) of the deep soil mixing samples at 7 and 28 days of the curing period were determined at the end of the test (Table 4).

In the statistical analysis, the significance level of the parameters affecting the performance of the deep mixing samples can be understood from the magnitude of the delta value in the response table obtained for the S/N ratios (larger is better-maximizing strength) and rank of parameters on UCS. The UCS generally increases while increasing cement and fly ash amounts and curing period since S/N ratios increase for all parameter levels (Table 5). Cement is the first, and fly ash is the second effective parameter on UCS as they are the main component in the hydration reaction by which soil particles bind together and produce a high strength structure. During the cement hydration, calcium ions are released then react with silica and alumina in soil. At the end of this process, pozzolanic products emerge and the strength increases. These pozzolanic products bind the clay particles together to form a new bonded, strong soil matrix [34]. The reactions between soil and calcium oxide (CaO) in cement and fly ash produce cementitious and pozzolanic gels such as C-S-H (calcium silicate hydrate gel) and C-A-S-H (calcium aluminate silicate hydrate gel). The increase in strength is related to the type and the number of possible reacting products. Therefore, the higher the content of calcium ions that exists in the binder, the higher strength is gained (Figure 2a).

The third efficient parameter on strength is the water content of the soil. Increasing its values maximizes UCS responses to a third level than the higher values of 28% water content of soil decreases UCS responses.

The water content of soil has little effect on the strength according to binders because the strength of samples primarily depends on the gel produced from the pozzolanic reactions. Therefore, the water content affects the strength indirectly by meeting the necessary moisture in the hydration reaction. The response of water content on strength depends on the water content needed for the applied binder contents. Each binder content has only one optimum water content. Fewer water contents lead to uncompleted hydration reaction and produce less gel causing a decrease in UCS. On the other hand, water amount over the optimum value cannot be absorbed during the hydration reaction. Therefore, it remains in the pores between soil particles causing larger voids at the microstructure. The optimum water content for mixing soil is the total water content by which the maximum strength is gained at a certain curing period [35]. The optimum water content was found by other researchers as the liquid limit of soil [36]. In this research, the optimum water content of soil-binder samples was 28% for silty soil since the liquid limit of the soil is 31%.

Table 4. Unconfined compression strength tests results for 7- and 28-days curing period

Design	7 days		28 days	
No	q_{u1} (kPa)	q_{u2} (kPa)	q_{u1} (kPa)	q_{u2} (kPa)
1	171	192	99	99
2	220	283	433	552
3	226	298	497	506
4	128	136	292	265
5	117	134	229	242
6	516	518	944	1041
7	834	967	1403	1061
8	1162	1079	1163	1695
9	303	274	513	521
10	777	942	1299	1342
11	743	760	1083	1319
12	1024	1281	1719	2083
13	1137	946	1161	966
14	1444	1337	1445	1337
15	1467	1917	1467	1917
16	2763	2460	2823	2459

Table 5. Response table for S/N ratios of UCS

Curing Period	Level	C	F	A	w/b	w_n
7 days	1	45.99	49.18	56.33	57.09	57.35
	2	54.08	55.96	53.95	56.72	56.16
	3	56.66	57.39	55.36	54.34	56.06
	4	64.03	58.24	55.13	52.61	51.19
	Delta	18.04	9.07	2.38	4.48	6.16
	Rank	1	2	5	4	3
28 days	1	49.17	50.54	57.47	57.54	57.50
	2	58.07	59.77	57.86	59.77	59.59
	3	60.96	60.49	58.56	58.07	60.01
	4	64.10	61.50	58.41	56.92	55.20
	Delta	14.94	10.96	1.09	2.85	4.82
	Rank	1	2	5	4	3

The effect of the water/binder ratio could be achieved according to the water content that had already been described above. It was concluded that the UCS decreases for both higher water content and higher water/binder ratios (Figure 2b).

The superplasticizer amount is the least effective parameter on UCS responses, but it was essential for the pumpability of binder grout consisting of high fly ash.

The regression equation established for the model created between UCS and design parameters was given in Equation (6) in coded units. Each parameter effect individually the UCS results and two- and three-parameter interactions were considered to increase the model quality. According to the statistical model, the values of R-sq., R-sq.(adj), and R-sq.(pred) were found 97.15%, 94.11%, and 93.04%, respectively. Concerning these very high regression qualities, the model created is accepted. Unconfined compression strength values of experimental results and predicted values according to regression analysis are given in Figure 3. There is a good conformity between the experimental and the predicted results: $q_{u,\ predicted}$=0.987$q_{u,\ experimental}$. These results are confirmed with other researchers for the feasibility and robustness of the Taguchi method [37,38] and desirability function approach [31,39].

$$q^{0.5} = -33.7 + 9.51C + 5.90F - 0.315A + 57.6(w/b) - 0.911w_n + 0.124P - 0.583CF - 7.1C(w/b) + 0.0014CP - 4.96F(w/b) + 0.0219FP + 0.560CF(w/b) - 0.00151CFP \quad (6)$$

3.2. Permeability test

Permeability tests were performed according to ASTM-D5084 [40]. After the soil-binder samples were placed into the cell of the triaxial compression test apparatus, the cell pressure and backpressure were applied as 500 kPa and 450 kPa, respectively. Experiments were repeated two times for each specimen. The permeability coefficient (k) of samples (Table 6) was calculated according to the following equation:

$$k = \frac{V \cdot L}{\Delta t \cdot A \cdot \Delta h} \quad (7)$$

where, V: volume of water leaking through the sample, L: specimen length, Δt: test duration, A: cross section area of specimen and Δh: head loss (height of water corresponds to back pressure since water pressure at outlet is zero).

In the S/N analysis, factors affecting the permeability coefficient (k) of the deep mixing samples are ranked as fly ash, cement, water/binder ratio, water content of the soil, and superplasticizer additive for 7 day-cured samples. At the end of the 28 days, the rank of parameters affecting k is water/binder ratio, water content of the soil, fly ash, superplasticizer additive, and cement (Table 7).

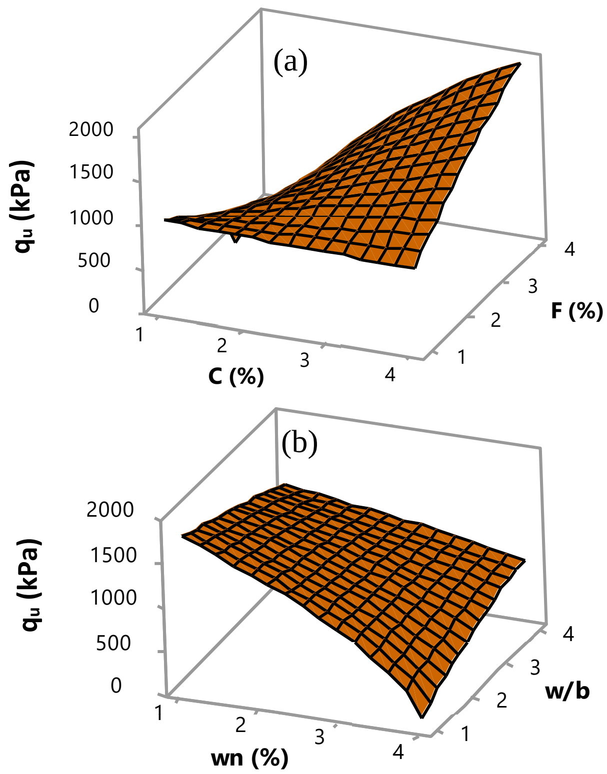

Figure 2. Surface plot of q_u vs a) cement and fly ash, b) water content and water/binder ratio

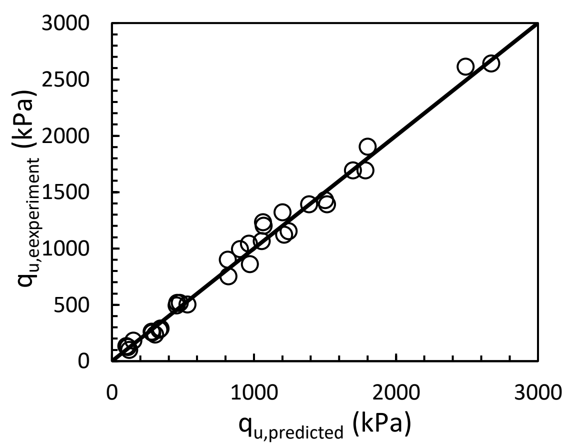

Figure 3. Unconfined compression strength values of experimental results and predicted values according to regression analysis

Permeability could change in different ways according to each parameter and its levels. Increasing cement content could affect permeability in two different ways. The first effect is decreasing permeability due to cement hydration because pozzolanic products bind the soil particles and decrease voids between them. The second effect is increasing the permeability by increasing the water amount in the sample, which causes more voids within the solid particles. According to their combined effects, the permeability could increase or decrease. As the permeability decreased from level 1 till level 2, the decrease in voids due to pozzolanic products was higher than the increase in voids due to the excess water amount. Between the 2nd and the 3rd levels of cement, the permeation increased massively because the increase in voids due to excess water was larger with respect to the decrease in voids due to pozzolanic products. Over the 3rd level of cement content, the permeability decreases again according to the increase in cement content. The decrease in voids due to pozzolanic products was larger than the increase in voids due to water excess. The fly ash amount also shows the same effects on permeability. Increasing fly ash content results in a decrease in permeability. Increasing fly ash content over the 2nd level up to the 3rd level resulted in a massive increase in permeability which means that the increase in voids due to water excess was very large with respect to the decrease in voids due to pozzolanic products. Finally, the increase in fly ash content from the 3rd up to the 4th level resulted in a little decrease in permeability with respect to the previous increase. In this period, the decrease in voids due to pozzolanic products was larger than the increase in voids due to water excess. The first two levels of the additive result in high permeability. On the other hand, the last two levels result in lower permeability. Therefore, the additive is accepted to be a permeability decreasing parameter. The water/binder ratio reduces the permeability until the third level. After that, the permeability starts to rise again while increasing the water/binder ratio over that level. For the water content, a similar effect was noticed as the permeability decreases while increasing water level till the second level. Then, it starts to rise again while increasing water over the second level till the fourth. In addition, the long curing periods result in lower permeability.

The regression equation is established for the model created between the coefficient of permeability and designing parameters as shown in Equation (8). This regression equation shows that the parameters have various effects on permeability. In addition, interactions of two and three parameters were included through the model for their high effects. According to the model, almost high regression quality ratios were found. The values of R-sq., R-sq.(adj), and R-sq.(pred) were obtained 96.41, 90.58, and 70.33, respectively. Concerning these high values, the model could be accepted. Permeability coefficient values of experimental results and predicted values according to regression analysis are given in Figure 4. There is a good agreement between the experimental results and the predicted values: $k_{,predicted}=0.864k_{,experimental}$.

$$\begin{aligned}-k^{-0.5} = {} & 69.3 - 15.19C - 6.98F + 0.16A - 127.7(w/b) \\ & + 1.305w_n + 0.14P + 0.914CF + 13.98C(w/b) \\ & - 0.0151CP + 6.77F(w/b) + 0.0294FP \\ & - 0.741CF(w/b) - 0.00500CFP \end{aligned} \quad (8)$$

3.3 Optimization

There are two types of optimizations; single response and multi-response optimizations. For single response optimizations, one optimal solution can be obtained. For multi-response optimizations, a set of optimal solutions would be found.

Table 6. Permeability tests results for 7- and 28-days curing period

Design No	7 days		28 days	
	k_1 (x10^{-9}) (m/s)	k_2 (x10^{-9}) (m/s)	k_1 (x10^{-9}) (m/s)	k_2 (x10^{-9}) (m/s)
1	1.790	1.730	2.230	2.200
2	0.479	0.301	0.813	0.674
3	2.370	2.180	1.040	1.180
4	1.400	0.951	7.370	7.060
5	1.550	1.320	0.753	0.673
6	0.417	0.393	2.890	2.680
7	6.260	6.280	1.040	1.040
8	1.360	1.320	1.820	1.780
9	1.500	1.440	0.937	0.956
10	1.780	1.790	0.778	0.793
11	23.10	22.80	2.760	2.680
12	14.60	12.70	1.110	1.010
13	0.500	0.500	0.618	0.604
14	2.110	2.120	1.040	1.050
15	10.70	10.70	13.30	12.60
16	2.010	2.070	0.937	0.942

Table 7. Response table for S/N ratios of k

Curing Period	Level	C	F	A	w/b	w_n
7 days	1	178.7	178.7	172.4	167.5	171.7
	2	176.6	181.1	170.4	176.1	175.7
	3	165.4	162.3	175.1	174.6	176
	4	173.2	171.8	175.9	175.6	170.4
	Delta	13.3	18.8	5.5	8.6	5.6
	Rank	2	1	5	3	4
28 days	1	174.4	180.2	174.0	178.0	172.0
	2	177.1	178.8	175.7	178.3	180.8
	3	178.3	172.0	178.5	181.2	178.5
	4	175.5	174.4	177.2	168.0	174.2
	Delta	3.9	8.2	4.5	13.1	8.9
	Rank	5	3	4	1	2

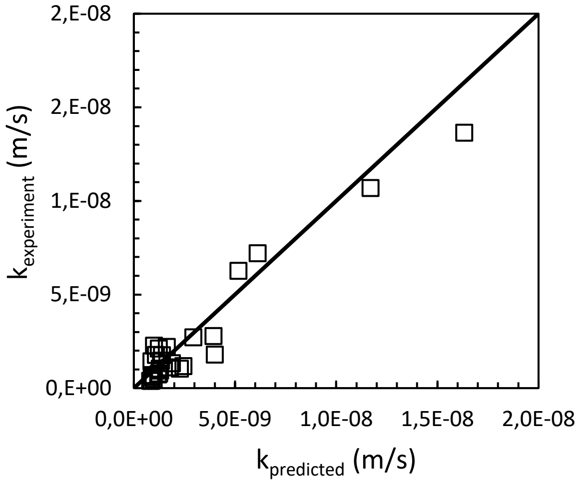

Figure 4. Permeability coefficient values of experimental results and predicted values according to regression analysis

In this study, two responses (q_u and k) were used because it was intended to construct the most durable and most impermeable deep mixing column. Therefore, optimum design parameters were obtained for maximizing q_u and minimizing k. The desirability function method was applied to find an optimal combination. The importance level of responses was chosen as 6 and 3 for q_u and k, respectively. The optimization plot of the two responses shows the parameter values of the optimal solutions (Figure 5). The vertical red lines represent the optimal values of parameters. The horizontal blue dashed lines represent the optimum response values (q_u=2821.5 kPa and k=8.82E-11 m/s). The black curves represent the desirability on the vertical axis and the parameter values on the horizontal axis. The value of composite desirability is 0.9998. The optimal parameter values are as followed; cement is 3.75 (14 %), fly ash is 3.80 (14 %), additive is 3.1212 (2.68 %), water/binder ratio is 1.25 (0.95), water content of untreated soil is 1.25 (21 %) and curing period is 2 (28 days). Cement and fly ash are responsible for producing gels to bind the soil particles and fill the voids between them. Therefore, the higher ratios of these two parameters can increase UCS and decrease the coefficient of permeability. According to these behaviors, higher values were chosen for binders in the present study as shown above. The optimum cement content is related to the stabilized soil type besides the requirements for the site [41]. Besides, different soils react differently to cementitious additives concerning the conditions of the site. They optimized the cement content for clay soil between 10%, 15%, and 20% of the dry weight of the clay. Replacing clay with fly ash in various ratios through 5, 10, 20, and 50% by dry weight of the total mixture, the load-bearing capacity of clay increase with the fly ash amount [42]. Yet fly ash contents from 20 to 50% didn’t improve the load-bearing capacity. As a result, the optimum fly ash content was accepted as %20. For binders, generally, these optimum amounts could change concerning the site conditions and the stabilized soil type as mentioned before. The UCS values are related to the molding water content [13]. There is an optimum value for each cement content. Besides, UCS response for water/binder ratios between 0.6 and 2, the curves between UCS against water are similar to the compaction curves between dry density and water content. The difference in UCS values depends only on the bonds resulting from the water available.

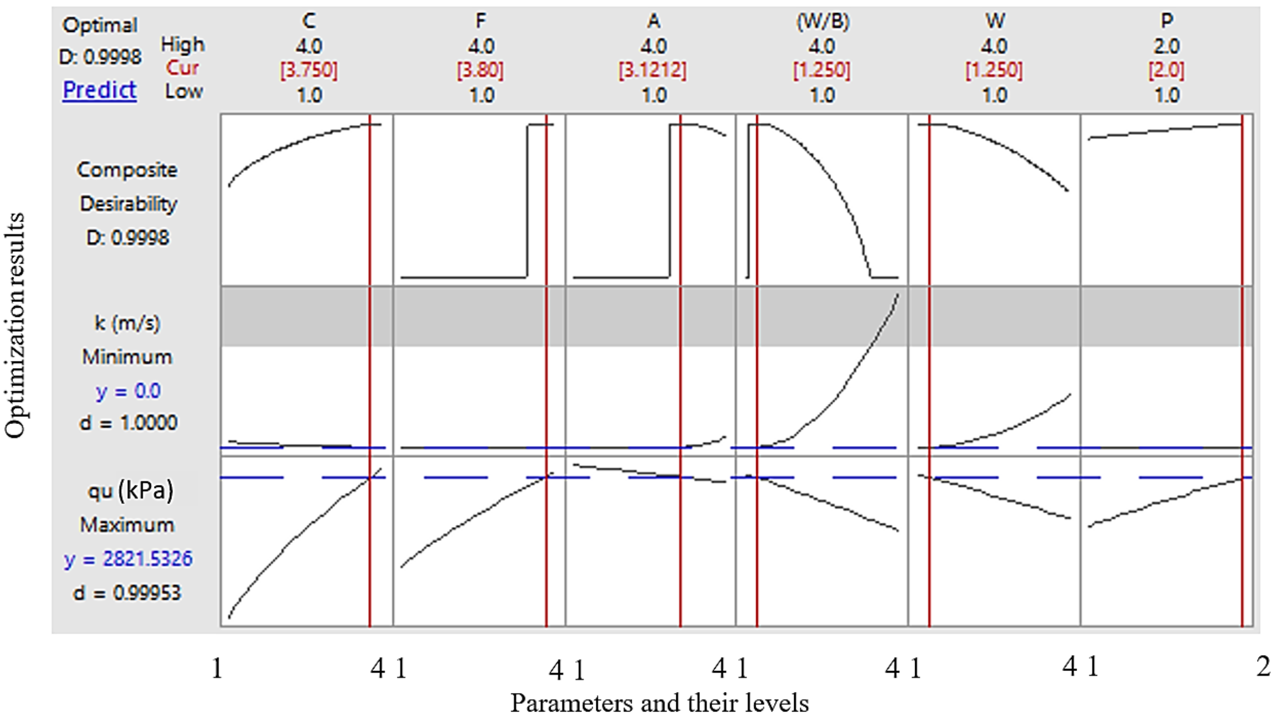

Figure 5. Optimization graphs for two responses

The addition of superplasticizers decreases yield value and plastic viscosity [43]. The arrangement of the particles within samples depends on the superplasticizer type. The w/c ratio has a significant effect on the performance of the superplasticizer because high w/c ratios decrease the performance of the superplasticizer. Superplasticizers can release water from the mixture. Therefore, more releases of water under higher dosages of superplasticizer could result in a great loss with the pozzolanic products and their gel causing more voids and less strength within the samples. This is why small dosages are applied generally like 1% by the weight of cementitious materials [16].

After selecting the optimal levels of each parameter, the last step is to predict and verify the values of the responses by using these optimal levels. For the unconfined compression strength, the error between experimental and predicted results was 3%, which means that the model is close to the real situation (Table 8). For the coefficient of permeability, the percentage of error was found a little bit higher as 13.5% which means that the developed model still includes some errors or another effective parameter should have been included in the developed model, or maybe there is an included parameter that misleads the prediction process.

3.4 Scanning Electron Microscopy (SEM) Analysis

Scanning electron microscope (SEM) analysis was performed to understand the microstructure of deep mixing samples. SEM images on untreated silty soil and soil-binder samples (design 9, design 11, and the optimum design) are given in Figure 6. The clear SEM images were obtained at 1000 magnifications. Untreated soil includes just minerals with voids caused by the irregularity of soil minerals (Figure 6a). In design 9, the microstructure of the soil-binder sample contains calcium silicate hydrate (C-S-H), calcium hydrate (C-H), and large voids (Figure 6b). The cement content of 11% produced C-S-H gels filling many voids and binding soil particles, however more voids were observed. In addition, many C-H particles were deposited on the surface of C-S-H gels as there weren't any fly ash particles. Therefore, the unconfined compression strength wasn't high enough. In design 9, the grains were accumulated separately leaving large voids. Such a structure could be classified as aggregated but deflocculated (FF associations).

In the microstructure of design 11, the formation of C-S-H gel, C-H, ettringite, and portlandite were observed (Figure 6c). By adding fly ash, the amount of C-S-H gels increases because of the reaction between C-H particles and fly ash.

Table 8. Experimental validation of the developed model with optimal parameters

Responses	Predicted	Experimental	Error
q_u (kPa)	2821.5	2737.1	3.0%
k (m/s)	8.82E-11	1.02E-10	13.5%

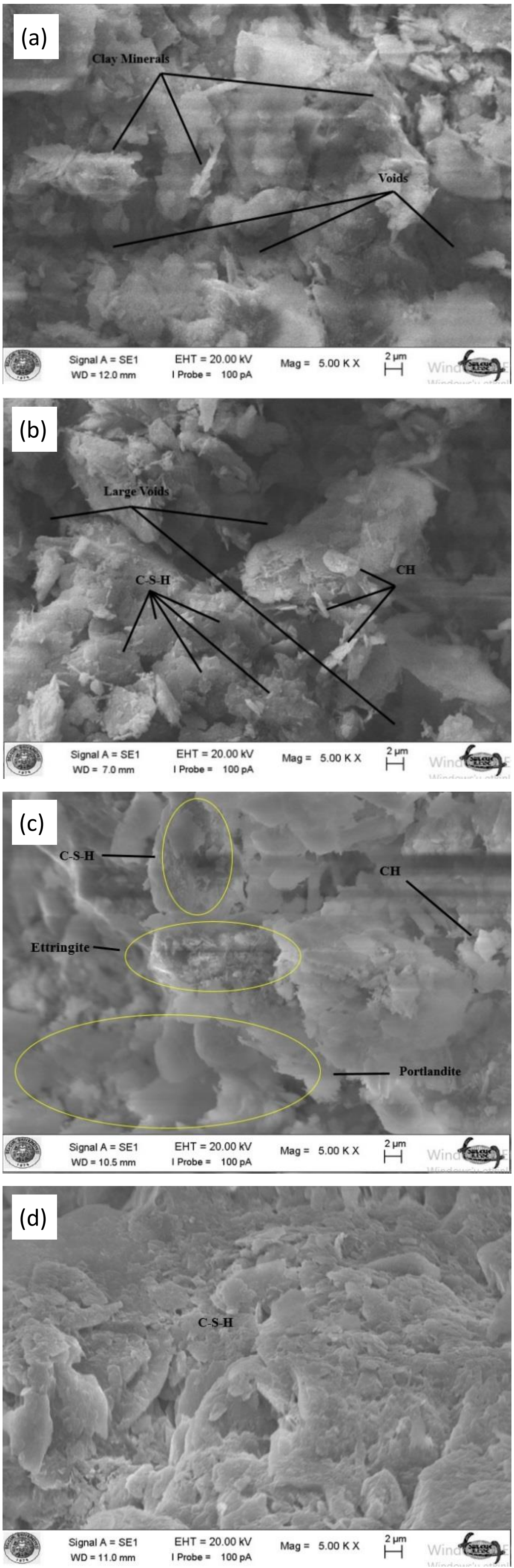

Figure 4. SEM images of a) untreated silty soil, b) design 9, c) design 11, and d) optimum design

Hence, fewer C-H particles were observed on the surface of C-S-H. Therefore, smaller voids and stronger bonds were obtained. Besides, ettringite between particles was very effective that high strength could be obtained. The formation of large portlandite particles was useful as it reduced the voids that existed within the microstructure because design 11 contains a continuous smooth face with fewer voids in between the particles. It could be classified as flocculated and aggregated (EE associations). In the microstructure of the optimum design, only C-S-H gel exists (Figure 6d). The aim of applying SEM analysis on the optimum design is to validate this model again for the formations at the microstructure. Almost all C-H particles were reacted with fly ash resulting in more C-S-H gels since the optimum content of fly ash was applied. Therefore, most of the voids were filled with C-S-H gels causing highly reduction in the permeability. Concerning the optimum design, all the particles are regularly connected, the surface has no roughness, and the particles are arranged in the same direction. Therefore, this structure could be classified as flocculated and aggregated (EE associations).

4. Conclusions

The effects of soil water content, cement, fly ash, superplasticizer contents, water/binder ratio, and curing period for soil-binder samples simulating deep mixing columns were studied by unconfined compression tests, permeability tests, and SEM analysis. Since there are so many parameters and levels to be researched, the design of the experiments was made according to the Taguchi method. The results were analyzed by S/N and regression analyzes, and then the optimization study was performed. While the amount of cement is effective in manufacturing durable columns, the amount of fly ash is effective in manufacturing impermeable columns. The increase in strength with cement content depends mainly on the cement hydration by which released calcium ions react with silica and alumina of the silty soil and form pozzolanic products. Increasing cement and fly ash content could affect the permeability in two different ways. The first effect is decreasing the permeability due to cement hydration because pozzolanic products bind the soil particles and decrease the void ratio. The second effect is increasing the permeability due to the higher water content causing more voids between particles. The first effect is more dominant for lower water/binder ratios and vice versa. The addition of superplasticizers decreases the flow consistency and the plastic viscosity. However, more dosages of superplasticizers could cause a great loss on forming the pozzolanic products.

In the optimum design of DMC having high strength and low permeability, grout content should be consisting of 14% cement, 14% fly ash, 2.68% superplasticizer additive, and 0.95 water/binder ratio. That is, 50% of the total dry binder amount is fly ash. This result shows that in soil improvement works with deep soil mixing method, the use of cement is reduced by 50% by using fly ash to produce more durable and more impermeable columns. One more binder silo can be installed on the construction site and the grout can easily be prepared with cement and fly ash. In this case, it is necessary to use the superplasticizer additive as the fly ash will increase the density and flow consistency of the grout. The additive can also be added to the grouting water and then added to the grout mixture.

Declaration

The author(s) declared no potential conflicts of interest with respect to the research, authorship, and/or publication of this article. The author(s) also declared that this article is original, was prepared in accordance with international publication and research ethics, and ethical committee permission or any special permission is not required.

Author Contributions

The authors carried out the investigation and co-designed the planning of the experiments. Y. Yenginar contributed to obtaining and interpreting the experimental and statistical results, writing and editing the article. A.A.M.M. Mobark contributed to the experimentation, literature review and writing original draft of article. M. Olgun contributed to the interpretation of the results, writing review of the article.

Reference

1. Shrestha R. and A. Al-Tabbaa, *Development of predictive models for cement stabilized soils*. In: *Proceedings of the Fourth International Conference on Grouting and Deep Mixing*, 2012: New Orleans, Louisiana, United States. p. 221–231.
2. Dias D.R., G. Camarini, and M.G. Miguel, *Preliminary laboratory tests to study the increase of strength in samples of soft soils with cement, for treatments using Dry-Mix System*. In: *Proceedings of the Fourth International Conference on Grouting and Deep Mixing*, 2012: New Orleans, Louisiana, United States. p. 454–462.
3. Li L., F. Santos, Y. Li, P.E.W. Shao, Q. Zhao, and F. Amini, *Evaluation of fly ash and soil mixtures for use in highway embankments*. In: *Geo-Congress: State of the Art and Practice in Geotechnical Engineering*, 2012: Oakland, California, United States. p. 3672–3680.
4. Ranga S.K., *Geotechnical characterization of soft clay treated with a bottom and fly ash mixture*. In: *Geo-China: Innovative Technologies for Severe Weather and Climate Change*, 2016: Shandong, China. p. 118–125.
5. Akash P., K. Arvind, G. Deepak, and P. Pankaj, *Compaction and strength behavior of tire crumbles–fly ash mixed with clay*. J. Mater. Civ. Eng., 2018. **30**(4): p. 1–9.
6. Show K., J. Tay, and A.T.C. Goh, *Reuse of incinerator fly ash in soft soil stabilization*. J. Mater. Civ. Eng., 2003. **15**(4): p. 335–343.

7. Kumar B.R.P. and R.S. Sharma, *Effect of fly ash on engineering properties of expansive soils*. J. Geotech. Geoenviron. Eng., 2004. **130**(7): p. 764–767.
8. Senol A., E. Etminan, and C.G. Olgun, *Stabilization of clayey soils using fly ash and homopolymerpolypropylene*. In: *Geo-Congress: State of the Art and Practice in Geotechnical Engineering*, 2012: Oakland, California, United States. p. 3929–3938.
9. Amadi A.A., A.O. Eberemu, and K.J. Osinubi, *Strength consideration in the use of lateritic soil stabilized with fly ash as liners and covers in waste landfills*. In: *Geo-Congress: State of the Art and Practice in Geotechnical Engineering*, 2012: Oakland, California, United States. p. 3835–3844.
10. Akbulut S. and A. Sağlamer, *Evaluation of fly ash and clay in soil grouting*. In: *Grouting and Ground Treatment*, 2003: New Orleans, Louisiana, United States. p. 1192–1199.
11. Jongpradist P., N. Jumlongrach, Y. Sompote, and S. Chucheepsakul, *Influence of fly ash on unconfined compressive strength of cement-admixed clay at high water content*. J. Mater. Civ. Eng., 2010. **22**(1): p. 49–58.
12. Zhang C., J. Yang, X. Ou, J. Fu, Y. Xie, and X. Liang, *Clay dosage and water/cement ratio of clay-cement grout for optimal engineering performance*. Applied Clay Science, 2018. **163**(1): p. 312–318.
13. Ribeiro D., R. Néri, and R. Cardoso, *Influence of water content in the UCS of soil-cement mixtures for different cement dosages*. In: Procedia Engineering. Elsevier Ltd., 2016. **143**(1): p. 59–66.
14. Azadi M.R., A. Taghichian, and A. Taheri, *Optimization of cement-based grouts using chemical additives*. Journal of Rock Mechanics and Geotechnical Engineering, 2017. **9**(4): p. 623–637.
15. Zhang Q., J. Liu, J. Liu, F. Han, and W. Lin, *Effect of superplasticizers on apparent viscosity of cement-based material with a low water–binder ratio*. J. Mater. Civ. Eng., 2016. **28**(9): p. 1–7.
16. Shaikh F.U. and S.W.M. Supit, *Effects of superplasticizer types and mixing methods of nanoparticles on compressive strengths of cement pastes*. J. Mater. Civ. Eng., 2016. **28**(2): p. 1–7.
17. Aita C.A.G., I.C. Goss, T.S. Rosendo, M.D. Tier, A. Wiedenhöft, and A. Reguly, *Shear strength optimization for FSSW AA6060-T5 joints by Taguchi and full factorial design*. Journal of Materials Research and Technology, 2020. **9**(6): p. 16072–9.
18. Voelkel J.G., *Fractional factorial designs*. *In: Encyclopedia of Statistics in Quality and Reliability*. 2008, Chichester, U.K.: John Wiley & Sons, Ltd.
19. Taguchi G. and S. Konishi, *Taguchi methods orthogonal arrays and linear graphs: Tools for quality engineering*. 1987, Dearborn, Michigan: Amer Supplier Inst.
20. Taguchi G., E.A. Elsayed, and T.C. Hsiang, *Quality engineering in production systems*. 1989, New York, N.Y.: McGraw-Hill.
21. Taguchi G., *Introduction to quality engineering: Designing quality into products and processes*. 4th ed. 1988, Tokyo: Asian Productivity Organization.
22. Taguchi G., S. Chowdhury, and Y. Wu. *Taguchi's Quality Engineering Handbook*. 2004, Hoboken, NJ, USA: John Wiley & Sons, Inc.
23. Tan Ö., *Investigation of soil parameters affecting the stability of homogeneous slopes using the Taguchi method*. Eurasian Soil Science, 2006. **39**(11): p. 1248–1254.
24. Tan Ö., A.S. Zaimoglu, S. Hinislioglu, and S. Altun, *Taguchi approach for optimization of the bleeding on cement-based grouts*. Tunnelling and Underground Space Technology, 2005. **20**(2): p. 167–173.
25. Wasantha P.L.P. and P.G. Ranjith, *The Taguchi approach to the evaluation of the influence of different testing conditions on the mechanical properties of rock*. Environmental Earth Sciences, 2014. **72**(1): p. 79–89.
26. Zhang F., M. Wang, amd M. Yang, *Successful application of the Taguchi method to simulated soil erosion experiments at the slope scale under various conditions*. CATENA, 2021. **196**:104835.
27. Özel S., E. Vural, and M. Binici, *Taguchi method for investigation of the effect of TBC coatings on Ni-Cr bond-coated diesel engine on exhaust gas emissions*. International Advanced Researches and Engineering Journal, 2020. **4**(1): p. 14–20.
28. ASTM C494/C494M−19, *Standard specification for chemical admixtures for concrete*. 2020, West Conshohocken, PA.
29. Derringer G. and R. Suich, *Simultaneous optimization of several response variables.* Journal of Quality Technology, 1980. **12**(4): p. 214–219.
30. Bouzid L., S. Berkani, M.A. Yallese, F. Girardin, and T. Mabrouki, *Estimation and optimization of flank wear and tool lifespan in finish turning of AISI 304 stainless steel using desirability function approach*. International Journal of Industrial Engineering Computations, 2018. **9**(1): p. 349–368.
31. Fitrianto A. and H. Midi, *Multi-response optimization via desirability function for the black liquor data*. Journal of Science and Technology, 2012. **4**(1): p. 91-101.
32. Sahoo A.K. and P.C. Mishra, *A response surface methodology and desirability approach for predictive modeling and optimization of cutting temperature in machining hardened steel*. International Journal of Industrial Engineering Computations, 2014. **5**(3): p. 407–416.
33. ASTM D2166-00, *Standard test method for unconfined compressive strength of cohesive soil*. 2000, West Conshohocken, PA.
34. Lorenzo G.A. and D.T. Bergado, *Fundamental characteristics of cement-admixed clay in deep mixing*. J. Mater. Civ. Eng., 2006. **18**(2): p. 161–174.
35. Bergado D.T. and G.A. Lorenzo, *Economical mixing method for cement deep mixing*. In: Innovations in Grouting and Soil Improvement, 2005: Austin, Texas, United States. p. 1–10.
36. Tastan E.O., T.B. Edil, C.H. Benson, and A.H. Aydilek, *Stabilization of organic soils with fly ash*. J. Geotech. Geoenviron. Eng., 2011. **137**(9): p. 819–833.
37. Uray E., Ö. Tan, S. Çarbaş, and İ.H. Erkan, *Metaheuristics-based pre-design guide for cantilever retaining walls*. Teknik Dergi, 2021. **32**(4): p. 10967–93.
38. Kate G.K., C.B. Nayak, and S.B. Thakare, *Optimization of sustainable high-strength–high-volume fly ash concrete with and without steel fiber using Taguchi method and multi-regression analysis*. Innovative Infrastructure Solutions, 2021. **6**(2): p. 1-18.
39. Şimşek B., Y.T. İç, E.H. Şimşek, *A full factorial design-based desirability function approach for optimization of properties of C 40/50 concrete class*. Mathematical and Computational Applications, 2013. **18**(3): p. 330–339.

40. ASTM D5084-16a. *Standard test methods for measurement of hydraulic conductivity of saturated porous materials using a flexible wall permeameter*. 2016, West Conshohocken, PA.

41. Fatahi B., D. Engelbert, S. Mujic, and H. Khabbaz, *Assessment of surcharging on strength and stiffness of cement treated clays*. In: *Proceedings of the Fourth International Conference on Grouting and Deep Mixing*, 2012: New Orleans, Louisiana, United States. p. 272–80.

42. Priyadarshee A., A. Kumar, D. Gupta, and P. Pushkarna, *Compaction and strength behavior of tire crumbles–fly ash mixed with clay*. J. Mater. Civ. Eng., 2018. **30**(4):04018033 p. 1-9.

43. Faroug F., J. Szwabowski, and S. Wild, *Influence of superplasticizers on workability of concrete*. J. Mater. Civ. Eng., 1999. **11**(2): p. 151-157.